Adaptive reduced basis strategy dedicated to the solution of nonstationary stochastic thermal problems

Benoit Magnain, Alain Batailly, Éric Florentin

Adaptive reduced basis strategy dedicated to the solution of nonstationary stochastic thermal problems

Benoît Magnain[1,*], Alain Batailly[2], Eric Florentin[1]

Abstract

This contribution addresses the modelling and the stochastic analysis of transient thermal processes by means of the finite element method. It focuses on the theoretical presentation as well as the application of an efficient reduced basis strategy that advantageously lowers the dimension of the investigated system. The modal content of the reduced basis is driven by the goal oriented error assessment of a user-defined quantity of interest. The first section of the article presents the stochastic system of interest: key aspects of a stochastic analysis are recalled along with the employed spatial discretization. The newly developed adaptive reduced basis strategy is then detailed in the second section before extensive numerical investigations are carried out in order to validate it in the last section of the article. A numerical benchmark allowing for the confrontation of the proposed strategy with usual Monte-Carlo simulations highlights the benefits of the method that allows for a precise control of the maximum admissible error on the quantity of interest.

Keywords

Reduced basis; Adaptivity; Stochastic modelling; Goal-oriented error assessment; Parametric uncertainties.

1 - INSA-CVL / Université d'Orléans - PRISME
88, Boulevard Lahitolle, F-18020 Bourges, France
* **Corresponding author**: Tel.: +33 248 484 093. E-mail address: benoit.magnain@insa-cvl.fr
2 - École polytechnique de Montréal - LAVA
C.P. 6079, Succ. Centre-ville, Montréal, Québec, CANADA

Bases réduites adaptatives pour la résolution de problèmes thermiques stochastiques instationnaires

Benoît Magnain[1,*], Alain Batailly[2], Eric Florentin[1]

Résumé

Cet article porte sur la modélisation et l'analyse stochastique de phénomènes thermiques transitoires par la méthode des éléments finis. Les développements effectués portent sur la présentation théorique et l'application d'une méthodologie efficace reposant sur l'utilisation de bases réduites et permettant ainsi une diminution de la dimension du système étudié. Le contenu modal de la base réduite est relié à l'évaluation d'erreur avec objectif d'une quantité d'intérêt choisie par l'utilisateur. La première section de l'article porte sur le système stochastique étudié, et permet un rappel des notions fondamentales associées à une analyse stochastique ainsi que des bases de la procédure de discrétisation spatiale. Par la suite, la deuxième section présente en détail la méthodologie développée. Enfin, dans une dernière section, plusieurs calculs permettent de valider cette méthodologie. Un point de comparaison numérique entre la méthodologie proposée et des simulations de Monte-Carlo mettent en évidence les avantages de la méthode proposée notamment au niveau de la précision de l'erreur maximale admissible sur la quantité d'intérêt.

Mots-clés

Bases réduites; Adaptativité; Modélisation stochastique; Évaluation d'erreur sur une quantité d'intérêt; Incertitudes paramétriques

1 - INSA-CVL / Université d'Orléans - PRISME
88, Boulevard Lahitolle, F-18020 Bourges, France
* **Coordonnées**: Tel.: +33 248 484 093. Adresse courriel: benoit.magnain@insa-cvl.fr
2 - École polytechnique de Montréal - LAVA
C.P. 6079, Succ. Centre-ville, Montréal, Québec, CANADA

1. Introduction

Ever-growing computational power allows to simulate physical phenomena of increasing complexity. In particular, the use of fine spatial discretization for sophisticated multiphysics numerical simulations is now conceivable for deterministic systems. For stochastic systems however, obtaining relevant results from numerical simulations is still a challenge since a very large number of simulations must be carried out. The stochastic nature of a system may be related to uncertainties inherent to its manufacturing [1, 2] or to the fact that its solicitations—such as potential thermal gradients or pressure loads—are unknown.

There are two ways to model a stochastic problem: (1) one may consider a nonparametric probabilistic approach where the link between the values of the parameters and the mechanical model is not explicit as the one presented in [3] or (2) a parametric approach where the variability of design parameters is accounted for by means of parametric uncertainties may be employed. The method presented in this paper belongs to the second category. In any case, a stochastic system features a randomness that can only be accounted for with a statistically relevant sample thus implying a very significant increase in terms of computational costs. A state of the art of stochastic numerical methods can be found in [4, 5, 6] and references therein. These methods, most of which rely on the

well-known finite element method (FEM), may be split in three categories :

intrusive stochastic techniques are a generalization of the FEM accounting for uncertainties associated with the parameters of the problem. Both the variation of usual deterministic variables—space and time coordinates—and the random stochastic variables are discretized using the standard approach in the FEM: the Galerkin formulation [7, 8, 9, 10]. The cornerstone of these methods lies in a proper definition of the approximation space of the stochastic variables. As a downside, these methods are computationally expensive and their implementation may be arduous. In order to overcome the high computational cost of these techniques, specific developments are available in the literature such as (1) iterative methods well-matched to the structure of resulting matrices [11, 12, 13] and (2) the use of reduced bases in order to represent the random space [9, 14, 15];

non-intrusive stochastic techniques are widely used as they rely on typical deterministic computations. Indeed, the randomness of the system is accounted for by means of Monte Carlo simulations. A large number of deterministic problems are solved through out the random space [16]. Such an approach is conceptually simple, robust and easy to implement but requires solving a large number of finite element problems in order to generate an output sample that is statistically relevant. The increased computation time inherent to such methods may be mitigated by the use of a reduced basis. In [17, 18, 19], the authors introduced a reduced basis methodology to reduce the cost of Monte Carlo simulations, offering an attractive framework for solving stochastic problems with a large number of parameters. The idea is simple and effective because the different Monte Carlo shots lead to similar FE problems and therefore the reduced basis approach is highly performant.

Uncertainty quantification techniques may introduce further an estimation of the analysis. Different methods have been proposed to control the approximations, see for example [20, 21, 22, 23].

The method presented in this article can be classified as a non-intrusive technique. Indeed, it does not require any modification of the finite element formulation. However, and contrary to a classical Monte-Carlo approach, it does impose a very specific solution algorithm. It builds up on the idea of using a reduced basis combined with a goal oriented error assessment criterion which controls the content of the reduced basis in order to maximize its numerical efficacy. The present investigation is an extension of the work initiated in [24, 25] to transient thermal processes [26, 27]. As a matter of fact, the time dependence of the investigated problem makes it more arduous to solve. Indeed, the methodology introduced in [24] is specific to stationnary problems: assessing its applicability and relevance in the case of nonstationnary problems is the focus of this article.

In the first section of this article, the investigated thermal problem is presented in details: transient thermal equations are given before a brief description on how to tackle a stochastic problem with the usual Monte-Carlo strategy. In the second section, the proposed numerical strategy based on adaptive reduced basis is exposed. Theoretical details are given with respect to the problem formulation, the general algorithm and the error assessment procedure. In the last section of the article, numerical results are presented for a benchmark test: both the accuracy and the efficacy of the proposed numerical strategy are thoroughly analyzed.

2. Stochastic problem

Governing equations

We consider a bounded domain Ω, representing a 2D structure. The boundary $\partial\Omega$ of Ω, is divided in two parts $\partial_D\Omega$ and $\partial_N\Omega$ such that $\partial_D\Omega \cup \partial_N\Omega = \partial\Omega$ and $\partial_D\Omega \cap \partial_N\Omega = \varnothing$.

The employed material model is assumed to be isotropic with no temperature dependence. Relevant material parameters mentioned in the following include: the density ρ, the specific heat c and the thermal conductivity λ. The stochastic behavior of the model is introduced assuming that $\lambda(\mathbf{x}, \theta)$ is a random field, where $\mathbf{x} \in \Omega$ stands for the position vector, and $\theta \in \Theta$ characterizes the randomness. The sample space Θ is the set of possible outcomes of θ. As a random field, $\lambda(\mathbf{x}, \theta)$ is a function mapping each point vector $\mathbf{x}$ to a random variable, typically with all the same Probability Density Function (PDF) and with cross-correlation depending on the distance between the locations. Assuming that the spatial correlation is regular enough, the Karhunen-Loève decomposition [28, 29] allows for a representation of a random field by a sum of independent scalar random variables multiplied by deterministic functions of $\mathbf{x}$.

A prescribed flux field $\mathbf{f}_d$ is applied on $\partial_N\Omega$, a prescribed temperature field T_d is imposed on $\partial_D\Omega$ and a prescribed source field $\mathbf{r}_d$ is applied on Ω. In a general context, the material properties characterized by ρ, c and λ as well as the loadings $\mathbf{f}_d$, T_d and r_d may be random fields. Without loss of generality, it is assumed in the following that the randomness is restricted to the material parameters introduced in the thermal conductivity λ. Thus, the problem reads: find the unknown temperature field $T(\mathbf{x}, t, \theta)$ such that

$$
\begin{cases}
\operatorname{div}\left[\lambda(\mathbf{x},\theta)\mathbf{grad}\left(T(\mathbf{x},t,\theta)\right)\right] + r_d(\mathbf{x},\theta) = \rho(\mathbf{x},\theta)\, c(\mathbf{x},\theta)\, \dfrac{\partial T}{\partial t}(\mathbf{x},t,\theta) & \text{in } \Omega & \text{(1a)} \\
\mathbf{grad}\left(T(\mathbf{x},t,\theta)\right).\mathbf{n} = \mathbf{f}_d(\mathbf{x},t,\theta) & \text{on } \partial_N\Omega & \text{(1b)} \\
T(\mathbf{x},t,\theta) = T_d(\mathbf{x},t,\theta) & \text{on } \partial_D\Omega & \text{(1c)} \\
T(\mathbf{x},t=0,\theta) = T_0(\mathbf{x},\theta) & \text{on } \Omega & \text{(1d)}
\end{cases}
$$

In the remainder, $\mathcal{T}$ refers to the set of admissible temperatures $T(\mathbf{x}, t, \theta) \in \mathcal{T}$, satisfying (1c) and (1d).

Quantity of interest

The purpose of the stochastic analysis is to determine reliable statistical information of a response quantity of Interest I. Note that since the solution $T(\mathbf{x}, t, \theta)$ is a random field, any output computed from this solution is a random quantity, and therefore the statistics of this output (expected value, variance…) are the relevant information to be estimated. In this article, the assumption is made that the quantity of interest may be expressed as a scalar quantity linearly dependent on $T(\mathbf{x}, t, \theta)$: The purpose of the stochastic

analysis is to determine reliable statistical information of a response quantity of Interest I. Note that since the solution $T(\mathbf{x}, t, \theta)$ is a random field, any output computed from this solution is a random quantity, and therefore the statistics of this output (expected value, variance...) are the relevant information to be estimated. In this article, the assumption is made that the quantity of interest may be expressed as a scalar quantity linearly dependent on $T(\mathbf{x}, t, \theta)$:

$$I(\theta) = \ell_I(T(\mathbf{x}, t, \theta)), \tag{2}$$

where $\ell_I(\cdot)$ is a deterministic linear functional.

Reference solution

A reference solution is obtained using a non-intrusive approach that decouples the discretization of the physical space and the stochastic space, represented here by Ω and Θ. This can be described in two steps:

1. First, a few simplifications are introduced in order to solve the problem (1) and to obtain a numerical approximation of $T(\mathbf{x}, t, \theta)$ for a realization of θ (freezing the randomness):
   - *Karhunen-Loève truncation (section 2.3.1):* the Karhunen-Loève infinite expansion is approximated by limiting the sum to a finite number of terms, N_{KL},
   - *spatial discretization (section 2.3.2):* the problem (1) is approximated as the application of the FEM yields a spatially discrete system,
   - *time discretization (section 2.3.3)* is operated by means of the Crank-Nicholson time integration scheme.
2. Then, N_{MC} Monte Carlo simulations $\{\theta_k\}_{k=1,\dots,N_{\text{MC}}}$ are used to obtain an approximation of the probability density function of the quantity of interest $I(\theta)$.

Details of each of the aforementioned steps are given hereafter.

Karhunen-Loève truncation

The conductivity $\lambda(\mathbf{x}, \theta)$ of the system is a scalar function defined at each point of the continuous domain, and thus consists of an infinite number of usually correlated random variables. For computational purposes, $\lambda(\mathbf{x}, \theta)$ is discretized: it is expressed as a finite number of uncorrelated random variables by means of the truncated Karhunen-Loève decomposition [28, 29].

The definition of $\lambda(\mathbf{x}, \theta)$ is related to the value of the mean field $\lambda_0(\mathbf{x})$ and its covariance operator $\mathcal{C}(\mathbf{x}, \mathbf{x}')$:

$$\mathcal{C}(\mathbf{x}, \mathbf{x}') = \text{cov}(\lambda(\mathbf{x}, \theta), \lambda(\mathbf{x}', \theta)) \tag{3}$$

Assuming that the covariance operator $\mathcal{C}(\mathbf{x}, \mathbf{x}')$ is regular enough, the Karhunen-Loève decomposition yields a representation of $\lambda(\mathbf{x}, \theta)$ as a sum of mutually uncorrelated random variables multiplied by deterministic functions of $\mathbf{x}$:

$$\lambda(\mathbf{x}, \theta) = \lambda_0(\mathbf{x}) + \sum_{i=1}^{+\infty} \sqrt{\psi_i}\lambda_i(\mathbf{x})\xi_i(\theta) \tag{4}$$

where $\lambda_i(\mathbf{x})$ and ψ_i, $i = 1, 2, \dots$, are respectively the eigenfunctions and eigenvalues of the covariance operator $\mathcal{C}(\mathbf{x}, \mathbf{x}')$. The sum in Eq. (4) is then truncated after the first N_{KL} uncorrelated random variables $\xi_i(\theta)$, $i = 1, \dots N_{\text{KL}}$:

$$\lambda(\mathbf{x}, \theta) = \lambda_0(\mathbf{x}) + \sum_{i=1}^{N_{KL}} \sqrt{\psi_i}\lambda_i(\mathbf{x})\xi_i(\theta), \tag{5}$$

In the end, the investigated problem (1) becomes a stochastic problem of finite dimension.

Spatial discretization

The well-known finite element method is employed in order spatially discretize the temperature field $T(\mathbf{x}, t, \theta)$. The shape functions $N_i(\mathbf{x})$, $i = 1, \dots N_{dof}$ span the solution space $\mathcal{T}_h \subset \mathcal{T}$:

$$\mathcal{T}_h = \text{span}\left\{N_1, N_2, \dots, N_{N_{dof}}\right\}. \tag{6}$$

Accordingly, the numerical approximation of $T(\mathbf{x}, t, \theta_k)$ in $\mathcal{T}_h$ is:

$$T_h(\mathbf{x}, t, \theta_k) = \sum_{i=1}^{N_{dof}} T_i(t, \theta_k)N_i(\mathbf{x}), \tag{7}$$

where $T_i(t, \theta_k)$, $i = 1, \dots, N_{dof}$ are the nodal values of the discrete temperature field. Introducing the global vector of unknowns:

$$\mathbf{T}(t, \theta_k) = [T_1(t, \theta_k),\, T_2(t, \theta_k),\, \dots,\, T_{N_{dof}}(t, \theta_k)]^\intercal \tag{8}$$

the corresponding discretized form of problem (1) may be written in a matrix form :

$$\mathbb{C}(\theta_k)\,\mathbf{T}(t, \theta_k) + \mathbb{M}\,\dot{\mathbf{T}}(t, \theta_k) = \mathbf{F}(t), \tag{9}$$

where $\mathbb{C}$ is the conductivity matrix, $\mathbb{M}$ is the capacity matrix, $\mathbf{F}$ is the nodal flux vector.

For a given realization, the discretization error $T(\mathbf{x},t,\theta_k) - T_h(\mathbf{x},t,\theta_k)$ is intimately related to the definition of the spatial discretization $\mathcal{T}_h$ and its dimension N_{dof}, see Eq. (6). If attention is paid to refining the spatial discretization in appropriate areas, this error may be significantly decreased. Many techniques may be used in order to estimate the discretization error [30, 31, 32] but such estimation goes beyond the scope of this study. In the following, the assumption is made that the discretization error is small enough thus the presented numerical strategy is not influenced by it. That is the reason why the finite element approximation of the temperature field $T_h(\mathbf{x},t,\theta_k)$ is now used indifferently instead of its continuous counterpart $T(\mathbf{x},t,\theta_k)$.

Time integration scheme

The numerical solution of Eq. (9) calls for a discretization of the time interval $[0, t_f]$. To this end, the sequence of discrete time steps t_n, $n = 0, \dots N$ is introduced, with:

$$t_n = n\Delta t \quad \text{and} \quad N = \frac{t_f}{\Delta t} \tag{10}$$

the notation of related nodal temperature vectors is then simplified:

$$\mathbf{T}(t_n,\theta_k) = \mathbf{T}_n(\theta_k) \tag{11}$$

In the end, the numerical problem (9) to be solved sums up to:

$$\mathbb{C}(\theta_k)\,\mathbf{T}_n(\theta_k) + \mathbb{M}\,\dot{\mathbf{T}}_n(\theta_k) = \mathbf{F}_n, \quad n \in [0,N], \tag{12}$$

A direct time integration scheme is used for the solution of Eq. (12). It is based on the following approximation, which depend on a parameter γ :

$$\gamma\dot{\mathbf{T}}_{n+1}(\theta_k) + (1-\gamma)\dot{\mathbf{T}}_n(\theta_k) \approx \frac{\mathbf{T}_{n+1}(\theta_k) - \mathbf{T}_n(\theta_k)}{\Delta t}, \quad \gamma \in [0,1] \tag{13}$$

The introduction of Eq. (13) within Eq. (12) yields the linear system of equations:

$$\left(\frac{1}{\Delta t}\mathbb{M} + \gamma\mathbb{C}(\theta_k)\right)\mathbf{T}_{n+1}(\theta_k) - \left(\frac{1}{\Delta t}\mathbb{M} + (\gamma-1)\mathbb{C}(\theta_k)\right)\mathbf{T}_n(\theta_k) = \gamma\mathbf{F}_{n+1} + (\gamma-1)\mathbf{F}_n \tag{14}$$

that may be written in a contracted form:

$$\mathbb{X}(\theta_k)\mathbf{T}_{n+1}(\theta_k) - \mathbb{Y}(\theta_k)\mathbf{T}_n(\theta_k) = \mathbf{Z}_{n+1} \tag{15}$$

where:

$$\mathbb{X}(\theta_k) = \left(\frac{1}{\Delta t}\mathbb{M} + \gamma\mathbb{C}(\theta_k)\right) \tag{16}$$

$$\mathbb{Y}(\theta_k) = \left(\frac{1}{\Delta t}\mathbb{M} + (\gamma-1)\mathbb{C}(\theta_k)\right) \tag{17}$$

$$\mathbf{Z}_{n+1} = \gamma\mathbf{F}_{n+1} + (\gamma-1)\mathbf{F}_n \tag{18}$$

Initial conditions (1d) give $\mathbf{T}_0(\theta_k)$ while boundary conditions and external loads definition (1b) allow for obtaining $\mathbf{F}_n$ and $\mathbf{F}_{n+1}$. The time evolution of the nodal temperature field may then be achieved through the sequential solution of linear systems:

$$\mathbf{T}_{n+1}(\theta_k) = \mathbb{X}^{-1}(\theta_k)\left(\mathbf{Z}_{n+1} + \mathbb{Y}(\theta_k)\mathbf{T}_n(\theta_k)\right), \quad n \in [1,N] \tag{19}$$

The nature of the time integration scheme depends on the value of parameter γ :

- $\gamma = 0.0$: explicit Euler method
- $\gamma = 0.5$: Crank-Nicholson method
- $\gamma = 1.0$: implicit Euler method

In the following, the Crank-Nicholson method is used: $\gamma = 0.5$, it is a second-order unconditionally stable time integration scheme.

Monte-Carlo simulations

Monte-Carlo simulations rely on the generation of a large number N_{MC} of realizations of θ, namely $\{\theta_k\}_{k=1,\dots,N_{\text{MC}}}$. Then, the aggregation of each solution $\{T_h(\mathbf{x},t,\theta_k)\}_{k=1,\dots,N_{\text{MC}}}$ yields the approximation of the statistics of the quantity of interest $I(\theta)$.

In the context of the considered thermal problem, N_{MC} realizations of $\mathbb{C}(\theta)$ are generated using independent realizations of the random variables $\{\xi_i(\theta)\}_{i=1,\dots,N_{\text{KL}}}$, see (5). Subsequently, temperature fields $\{T_h(\mathbf{x},t,\theta_k)\}_{k=1,\dots,N_{\text{MC}}}$ are obtained by solving N_{MC} linear systems (9). The probability density function (PDF) of $I(\theta)$ is then characterized by its expectation $\mathbb{E}$ and variance $\mathbb{V}$ as:

$$\mathbb{E}[I(\theta)] \approx \frac{1}{N_{\text{MC}}}\sum_{k=1}^{N_{\text{MC}}} I(\theta_k) \quad , \quad \mathbb{V}[I(\theta)] = \mathbb{E}\left[I(\theta)^2 - \mathbb{E}[I(\theta)]^2\right] \tag{20}$$

Algorithm 1 sums up the procedure used for carrying out the Monte-Carlo simulations.

Data: the realizations $\{\theta_k\}_{k=1,\dots,N_{\mathrm{MC}}}, \gamma, \Delta t, t_f, \mathbb{C}_i, \mathbb{M}, \mathbf{F}(t), \mathbf{T}_0$
Result: A number of N_{MC} realizations of the quantity of interest, $I_{MC}(\theta_k)_{k=1,\dots,N_{\mathrm{MC}}}$
for $i = 1, \dots, N_{\mathrm{KL}}$ **do**
  Compute $\mathbb{C}(\theta_k) = \mathbb{C}_0 + \sum_{i=1}^{N_{\mathrm{KL}}} \sqrt{\psi_i}\mathbb{C}_i\xi_i(\theta_k)$;
  Compute $\mathbb{X}(\theta_k) = \left(\frac{1}{\Delta t}\mathbb{M} + \gamma\mathbb{C}(\theta_k)\right)$;
  Compute $\mathbb{Y}(\theta_k) = \left(\frac{1}{\Delta t}\mathbb{M} + (1-\gamma)\mathbb{C}(\theta_k)\right)$;
  for $n = 0, \dots, N$ **do**
    Compute $\mathbf{Z} = \gamma\mathbf{F}_{n+1} + (\gamma - 1)\mathbf{F}_n$;
    Compute $\mathbf{T}_{n+1}$ solving $\mathbf{T}_{n+1}(\theta_k) = \mathbb{X}^{-1}(\theta_k)\left(\mathbf{Z} + \mathbb{Y}(\theta_k)\mathbf{T}_n(\theta_k)\right)$;
  end
end

Algorithm 1: Monte-Carlo simulations algorithm

3. Proposed adaptive reduced basis strategy

The proposed adaptive reduced basis strategy aims at obtaining the N_{MC} realisations of the quantity of interest $\{I_{RB}(\theta_k)\}_{k=1,\dots,N_{\mathrm{MC}}}$ through the solution of Eqs. (2.3.1), (2.3.2) and (2.3.3) without time-consuming Monte-Carlo simulations. The system to be solved is projected onto a space of lower dimension by means of a dedicated reduced basis. The dimension of the basis is adjusted automatically in order to satisfy a user-defined criterion on the accuracy of each solution. The solution of each realization is thus approximated by a linear combination of the vectors contained in the reduced basis which are the solutions of N_{RB} carefully selected other realizations. The specificity of the proposed strategy lies in the adjustment of the reduced basis content. It is based on an error assessment criterion over the quantity of interest I.

New time formulation of the discretized problem

The solution of Eq. (15) over N time steps sums up to:

$$\begin{cases} \mathbb{X}(\theta_k)\mathbf{T}_1(\theta_k) - \mathbb{Y}(\theta_k)\mathbf{T}_0(\theta_k) &= \mathbf{Z}_1 \\ \mathbb{X}(\theta_k)\mathbf{T}_2(\theta_k) - \mathbb{Y}(\theta_k)\mathbf{T}_1(\theta_k) &= \mathbf{Z}_2 \\ \vdots & \\ \mathbb{X}(\theta_k)\mathbf{T}_N(\theta_k) - \mathbb{Y}(\theta_k)\mathbf{T}_{N-1}(\theta_k) &= \mathbf{Z}_N \end{cases} \tag{21}$$

which may be written using a matrix form:

$$\begin{pmatrix} -\mathbb{Y}(\theta_k) & \mathbb{X}(\theta_k) & 0 & \cdots & \cdots \\ 0 & -\mathbb{Y}(\theta_k) & \mathbb{X}(\theta_k) & 0 & \cdots \\ \vdots & \vdots & \vdots & \vdots & \vdots \\ \cdots & \cdots & 0 & -\mathbb{Y}(\theta_k) & \mathbb{X}(\theta_k) \end{pmatrix} \begin{bmatrix} \mathbf{T}_0(\theta_k) \\ \mathbf{T}_1(\theta_k) \\ \vdots \\ \mathbf{T}_N(\theta_k) \end{bmatrix} = \begin{bmatrix} \mathbf{Z}_1 \\ \mathbf{Z}_2 \\ \vdots \\ \mathbf{Z}_N \end{bmatrix} \tag{22}$$

Accounting for the initial conditions (1d) in this $N \times (N+1)$ matrix block system yields the non-symmetric $N \times N$ matrix block system:

$$\begin{pmatrix} \mathbb{X}(\theta_k) & 0 & \cdots & \cdots \\ -\mathbb{Y}(\theta_k) & \mathbb{X}(\theta_k) & 0 & \cdots \\ & \vdots & \vdots & \vdots \\ \cdots & 0 & -\mathbb{Y}(\theta_k) & \mathbb{X}(\theta_k) \end{pmatrix} \begin{bmatrix} \mathbf{T_1}(\theta_k) \\ \mathbf{T}_2(\theta_k) \\ \vdots \\ \mathbf{T}_N(\theta_k) \end{bmatrix} = \begin{bmatrix} \mathbf{Z}_1 + \mathbb{Y}(\theta_k)\mathbf{T}_0 \\ \mathbf{Z}_2 \\ \vdots \\ \mathbf{Z}_N \end{bmatrix} \tag{23}$$

For a given realization θ_k, $\tilde{\mathbf{T}}(\theta_k)$ and $\tilde{\mathbf{Z}}$ respectively represent the nodal temperature vector for each time step and the external loadings vector for each time step:

$$\begin{cases} \tilde{\mathbf{T}}(\theta_k) &= [\mathbf{T}_1(\theta_k)^\intercal, ..., \mathbf{T}_N(\theta_k)^\intercal]^\intercal \\ \tilde{\mathbf{Z}}(\theta_k) &= [\mathbf{Z}_1^\intercal + [\mathbb{Y}(\theta_k)\mathbf{T}_0]^\intercal, ..., \mathbf{Z}_N^\intercal]^\intercal \end{cases} \tag{24}$$

Using these notations, Eq. (23) may be simply written as:

$$\tilde{\mathbb{K}}(\theta_k)\tilde{\mathbf{T}}(\theta_k) = \tilde{\mathbf{Z}}(\theta_k) \tag{25}$$

where:

$$\tilde{\mathbb{K}}(\theta_k) = \begin{pmatrix} \mathbb{X}(\theta_k) & 0 & \cdots & \cdots \\ -\mathbb{Y}(\theta_k) & \mathbb{X}(\theta_k) & 0 & \cdots \\ & \vdots & \vdots & \vdots \\ \cdots & 0 & -\mathbb{Y}(\theta_k) & \mathbb{X}(\theta_k) \end{pmatrix} \tag{26}$$

Equation. (25) is then left multiplied by $\tilde{\mathbb{K}}(\theta_k)^\intercal$ in order to yield a symmetric matrix so that the system may be solved :

$$\left(\tilde{\mathbb{K}}(\theta_k)^\intercal \tilde{\mathbb{K}}(\theta_k)\right) \tilde{\mathbf{T}}(\theta_k) = \tilde{\mathbb{K}}(\theta_k)^\intercal \tilde{\mathbf{Z}}(\theta_k) \tag{27}$$

or:

$$\hat{\mathbb{K}}(\theta_k)\hat{\mathbf{T}}(\theta_k) = \hat{\mathbf{Z}}(\theta_k) \tag{28}$$

where $\hat{\mathbf{T}}(\theta_k) = \tilde{\mathbf{T}}(\theta_k)$ and $\hat{\mathbf{Z}}(\theta_k) = \tilde{\mathbb{K}}(\theta_k)^\intercal \tilde{\mathbf{Z}}(\theta_k)$. One may note that $\hat{\mathbb{K}}(\theta_k) = \tilde{\mathbb{K}}(\theta_k)^\intercal \tilde{\mathbb{K}}(\theta_k)$ is symmetric. On the base of Eq. (28), the following sections define the procedure for estimating the error associated with the use of a reduced basis.

Approximated solution using a reduced basis

Definition of the reduced basis

As in any other reduction technique, the construction of the reduced basis, namely $\mathbb{T}_{RB}$, is the cornerstone of the proposed numerical strategy since its dimension and its modal content respectively act upon the numerical efficacy and stability of the method. There is a wide variety of model reduced techniques that may be employed to build the reduced basis. One may mention the Proper Orthogonal Decomposition (POD) [33, 34] and the Reduced Basis method (RB) [35, 36]. These methods rely on a reduced basis computed once and for all. To the contrary, the particularity of the proposed reduced basis is that its modal content is not known *a priori*: it is enriched as soon as it is found inadequate to obtain an accurate solution for a given realization k.

For the first realization θ_1 of the system, the solution $\hat{\mathbf{T}}(\theta_1)$ is computed from Eq. (28). It is used as a starting point for the definition of the reduced basis :

$$\mathbb{T}_{RB} = \hat{\mathbf{T}}(\theta_1) \tag{29}$$

The basis $\mathbb{T}_{RB}$ is then progressively enriched for subsequent realizations θ_k every time the error criterion is not satisfied, see algorithm 2.

Reduced system

The definition of the reduced basis $\mathbb{T}_{RB}$ allows for the projection of the system to be solved (28) onto a reduced subspace by considering the following change of variables:

$$\hat{\mathbf{T}}_{RB}(\theta_k) = \sum_{i=1}^{N_{\mathrm{RB}}} a_i(\theta_k)\hat{\mathbf{T}}_i = \mathbb{T}_{RB}\,\mathbf{a}(\theta_k) \tag{30}$$

Indeed, the combination of Eqs. (30) and (28) yields:

$$\hat{\mathbb{K}}(\theta_k)\mathbb{T}_{RB}\,\mathbf{a}(\theta_k) = \hat{\mathbf{Z}} \tag{31}$$

which, after left-multiplication by $\mathbb{T}_{RB}^\intercal$ leads to:

$$\mathbb{K}_{RB}(\theta_k)\,\mathbf{a}(\theta_k) = \mathbf{Z}_{RB} \tag{32}$$

where:

$$\mathbb{K}_{RB}(\theta_k) = \mathbb{T}_{RB}^\intercal \hat{\mathbb{K}}(\theta_k)\mathbb{T}_{RB} \quad \text{and} \quad \mathbf{Z}_{RB}(\theta_k) = \mathbb{T}_{RB}^\intercal \hat{\mathbf{Z}}(\theta_k) \tag{33}$$

is the reduced system to be solved.

Adaptive strategy using error assessment

As mentioned above, the quantity of interest I is linearly dependent on the temperature, see Eq. (2). It may thus be written as:

$$I(\theta_k) = \ell_I(T(\mathbf{x}, t, \theta_k)) = \hat{\mathbf{G}}^\intercal \hat{\mathbf{T}}(\theta_k) \tag{34}$$

where $\hat{\mathbf{G}}$ is the discrete operator (extractor) associated to the linear function ℓ_I. For instance, assuming the quantity of interest is the temperature of a given point at a certain time, the vector $\hat{\mathbf{G}}$ only contains one non-zero value (set to 1) located where the quantity of interest is in $\hat{\mathbf{T}}(\theta_k)$. If the quantity of interest is not localized on a single point and must be estimated over a specific domain, two strategies may be employed. (1) A *local* approach that ensures a great accuracy consists in running the same number of simulations as the number of quantities of interest. Since simulations may be carried out independently one from another, the whole process may be parallelized and thus yield practically no extra computational cost. (2) A *global* approach consists in running a single simulation considering a ponderated average of all the quantities of interest.

Similarly to Eq. (34), the temperature computed from the reduced space may be written:

$$I_{RB}(\theta_k) = \ell_I(T_{RB}(\mathbf{x}, t, \theta_k)) = \hat{\mathbf{G}}^\intercal \hat{\mathbf{T}}_{RB}(\theta_k) \tag{35}$$

Consequently, the error $e(\theta_k)$ on the quantity of the interest for the realization θ_k is:

$$e(\theta_k) = I(\theta_k) - I_{RB}(\theta_k) = \hat{\mathbf{G}}^\intercal \left(\hat{\mathbf{T}}(\theta_k) - \hat{\mathbf{T}}_{RB}(\theta_k) \right) \tag{36}$$

In pratice, one can also define the relative error $e(\theta_k)/I(\theta_k)$. The introduction of the dual problem [37] related to the quantity of interest I for the reference problem (28) gives:

$$\hat{\mathbb{K}}(\theta_k)\hat{\mathbf{V}}(\theta_k) = \hat{\mathbf{G}} \tag{37}$$

where $\hat{\mathbf{V}}(\theta_k)$ is the solution of the dual problem. The combination of Eqs. (36) and (37) yields:

$$\begin{aligned} e(\theta_k) &= \left(\hat{\mathbb{K}}(\theta_k)\hat{\mathbf{V}}(\theta_k) \right)^\intercal \left(\hat{\mathbf{T}}(\theta_k) - \hat{\mathbf{T}}_{RB}(\theta_k) \right) \\ &= \hat{\mathbf{V}}(\theta_k)^\intercal \left(\hat{\mathbb{K}}(\theta_k)^\intercal \hat{\mathbf{T}}(\theta_k) - \hat{\mathbb{K}}(\theta_k)\hat{\mathbf{T}}_{RB}(\theta_k) \right) \\ &= \hat{\mathbf{V}}(\theta_k)^\intercal \left(\hat{\mathbf{Z}}(\theta_k) - \hat{\mathbb{K}}(\theta_k)^\intercal \hat{\mathbf{T}}_{RB}(\theta_k) \right) \end{aligned} \tag{38}$$

For each realization θ_k, the only unknown in Eq. (38) is $\hat{\mathbf{V}}(\theta_k)$. While the calculation of $\hat{\mathbf{V}}(\theta_k)$ is possible using Eq. (37), it must be avoided since the dimension of this equation is identical to the initial system in Eq. (28). In order to minimize computation times, $\hat{\mathbf{V}}(\theta_k)$ is approximated as follows:

$$\hat{\mathbf{V}}(\theta_k) \approx \hat{\mathbf{V}}_0 = \hat{\mathbb{K}}_0^{-1}\hat{\mathbf{G}} \tag{39}$$

where $\hat{\mathbb{K}}_0$ is obtained with $\lambda(\theta_k) = \lambda_0$. In the end, the computation of the error $e(\theta_k)$ is approximated by:

$$e(\theta_k) \approx e_{RB}(\theta_k) = \hat{\mathbf{V}}_0^\intercal \left(\hat{\mathbf{Z}}(\theta_k) - \hat{\mathbb{K}}(\theta_k)^\intercal \hat{\mathbf{T}}_{RB}(\theta_k) \right) \tag{40}$$

In the following, such approximation is numerically validated in the context of small-amplitude randomness. The impact of the approximation presented in Eq. (39) has previously been assessed [25] and compared with a finer, but more costly, approximation. It was found that for small variations of the variability, the obtained results are identical.

Proposed algorithm

In the proposed approach, the only user-defined parameter is the precision criterion ϵ_0 on the quantity of interest. This parameter controls the enrichment of the reduced basis in order to ensure that: $e_{RB}(\theta_k) \leq \epsilon_0$. The smaller ϵ_0, the higher the required precision and thus the larger becomes the reduced basis, automatically following algorithm 2. Previous sections are summarized in algorithm 2.

Data: the realizations $\{\theta_k\}_{k=1,\dots,N_{\text{MC}}}, \alpha, \Delta t, t_f, \mathbb{C}_i, \mathbb{M}, \mathbf{F}(t), \mathbf{T}_0, \hat{\mathbf{G}}, \epsilon_0$
Result: A number of N_{MC} realizations of the quantity of interest, $I_{RB}(\theta_k)_{k=1,\dots,N_{\text{MC}}}$
$N_{RB} = 1$ and compute $\mathbb{C}(\theta_1)$, $\mathbb{X}(\theta_1)$ and $\mathbb{Y}(\theta_1)$;
for $n = 0, \dots, N$ **do**
  Compute $\mathbf{Z} = \alpha \mathbf{F}_{n+1} + (\alpha - 1)\mathbf{F}_n$;
  Compute $\mathbf{T}_{n+1}$ solving $\mathbf{T}_{n+1}(\theta_1) = \mathbb{X}^{-1}(\theta_1)\left(\mathbf{Z} + \mathbb{Y}(\theta_1)\mathbf{T}_n(\theta_1)\right)$;
  Store $\hat{\mathbf{T}}(\theta_1)$ in $\mathbb{T}_{RB}$;
end
Compute and store $I_{RB}(\theta_1) = \hat{\mathbf{G}}^\intercal \hat{\mathbf{T}}(\theta_1)$;
Compute $\hat{\mathbf{V}}_0 = \hat{\mathbb{K}}_0^{-1}\hat{\mathbf{G}}$;
for $k = 2, \dots, N_{\text{KL}}$ **do**
  Compute $\mathbb{K}_{RB}(\theta_k)$ and $\mathbf{Z}_{RB}$ and solve $\mathbb{K}_{RB}(\theta_k)\mathbf{a}(\theta_k) = \mathbf{Z}_{RB}$;
  Compute $e_{RB}(\theta_k) = \hat{\mathbf{V}}_0^\intercal \left(\hat{\mathbf{Z}}(\theta_k) - \hat{\mathbb{K}}(\theta_k)^\intercal \hat{\mathbf{T}}_{RB}(\theta_k)\right)$ **if** $|e_{RB}(\theta_k)| > \epsilon_0$ **then**
    inadmissible solution;
    for $n = 0, \dots, N$ **do**
      Compute $\mathbf{Z} = \alpha \mathbf{F}_{n+1} + (\alpha - 1)\mathbf{F}_n$;
      Compute $\mathbf{T}_{n+1}$ solving $\mathbf{T}_{n+1}(\theta_k) = \mathbb{X}^{-1}(\theta_k)\left(\mathbf{Z} + \mathbb{Y}(\theta_k)\mathbf{T}_n(\theta_k)\right)$;
    end
    Compute and store $I_{RB}(\theta_k) = \hat{\mathbf{G}}^\intercal \hat{\mathbf{T}}(\theta_k)$;
    Store $\hat{\mathbf{T}}(\theta_k)$ in $\mathbb{T}_{RB}$ and $N_{\text{RB}} \leftarrow N_{\text{RB}} + 1$;
  else
    admissible solution;
    compute $\hat{\mathbf{T}}_{RB}(\theta_k) = \mathbb{T}_{RB}\,\mathbf{a}(\theta_k)$;
    Compute and store $I_{RB}(\theta_k) = \hat{\mathbf{G}}^\intercal \hat{\mathbf{T}}_{RB}(\theta_k)$;
    $\mathbb{T}_{RB}$ remains unchanged
  end
end

Algorithm 2: Proposed adaptive reduced basis algorithm

It should be underlined that $\hat{\mathbf{V}}_0$ is not computed based the first draw. Instead, it stems from the average value of the parameters. This is critical in order to ensure a proper estimation of the error. In addition, the sequence of draws is fully arbitrary. In previous work [25], several sequences are assessed and provide similar results. In its current implementation, the proposed methodology retains all admissible solutions within the reduced basis without any mathematical modification or optimization.

4. Numerical investigations

The numerical investigations carried out on a case study are twofold. In the first subsection, a reference solution using Monte-Carlo simulations is obtained. Then, in the following subsections, the proposed numerical strategy is applied and key points of the strategy such as the error assessment procedure is analyzed.

Description of the considered case study: deterministic problem

The following 2D case study is considered: a square domain of length $L_0 = 0.1$ m receives a constant heat flow $\phi = 300$ kW.m^{-2} on part of its edges, see Fig. 1, with $L_1 = 0.03$ m and $L_2 = 0.01$ m. There is no heat flow in any other part of the domain boundary: other edges are assumed perfectly adiabatic. The initial temperature T_0 is uniform across the domain: $T_0 = 0°$C. The system is investigated over $t_f = 120$ s, the time step of the Crank-Nicholson time integration scheme is $\Delta t = 1$ s. The domain is discretized by means of 2D four-node linear finite elements, the mesh is intentionally coarse (only 400 elements are used in total: 20 along each edge of the domain) in order to minimize computation times. The quantity of interest is the temperature in the middle of the domain after 120 s, that is $I = T(O, t_f) = T(\mathbf{x} = (0; 0), t = 120)$. The extractor (34) associated to I is a vector $\hat{\mathbf{G}}$ with a unique non null component (equals to one) corresponding to the node located on O and last time step.

The final temperature gradient in the domain for this deterministic system is depicted in Fig. 1 and the history of the temperature in the center of the domain $T(O, t)$ is shown in Fig. 2.

Reference solution of the stochastic problem

The material is assumed to be isotropic with the following properties: its density is $\rho = 7800$ kg·m^{-3} and its specific heat is $c = 700$ J·kg^{-1}·K^{-1}. The randomness of the system is introduced through its conductivity $\lambda(\mathbf{x}, \theta)$ defined by its mean value $\lambda_0 = 50$ W·m^{-1}·K^{-1} and its covariance operator $\mathcal{C}(\mathbf{x}, \mathbf{x}') = \alpha^2 e^{-\frac{\|\mathbf{x}-\mathbf{x}'\|}{a}}$. The random field $\lambda(\mathbf{x}, \theta)$ undergoes a Karhunen-Loève decomposition with 20 modes ($N_{\text{KL}} = 20$) and 10^5 realizations are considered ($N_{\text{MC}} = 10^5$). The severity of the problem, which is related to the amplitude of the randomness, is controlled by the two parameters a and α with $a \in \{0.25L_0; 0.5L_0; L_0\}$ and

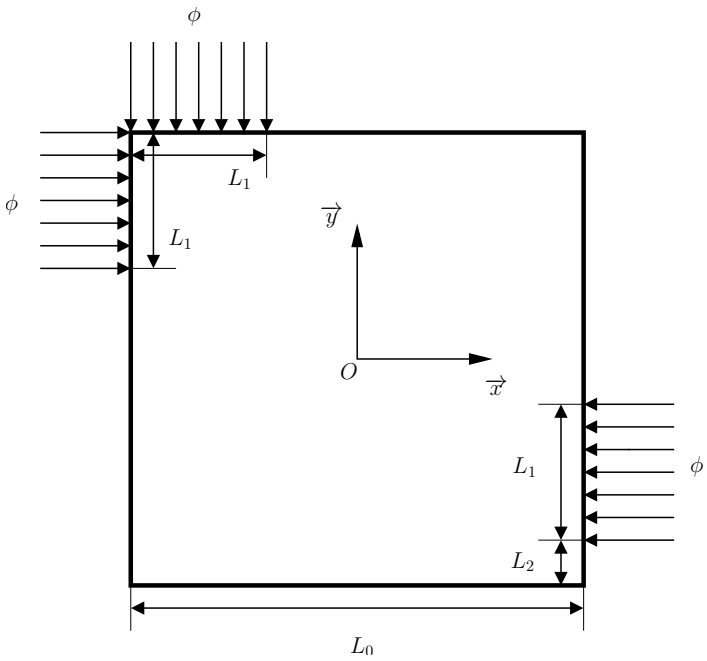

(a) boundary conditions

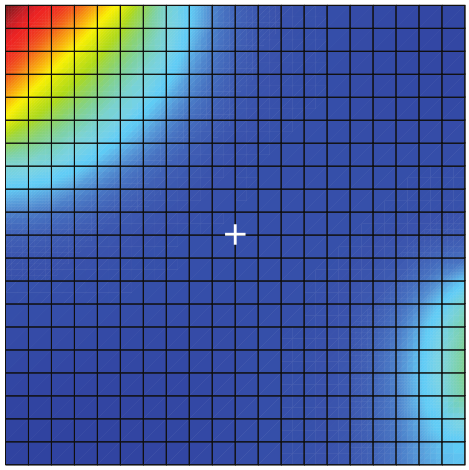

(b) temperature gradient ($t = t_f$) for uniform mean conductivity value λ_0

Figure 1. 2D test case

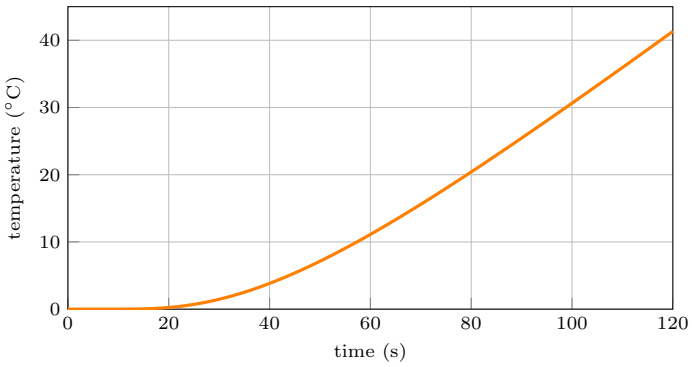

Figure 2. Temperature in the middle of the square domain: $T(O,t)$ for uniform mean conductivity value λ_0

$\alpha \in \{2\%; 5\%; 7\%\}$. In order to better apprehend the impact of the randomness on the quantity of interest, Tab. 1 features its expectation and standard deviation for different sets of parameters.

a	$0.25L_0$			$0.5L_0$			L_0		
α	2%	5%	7%	2%	5%	7%	2%	5%	7%
$\mathbb{E}[I(\theta)]$	41.3123	41.2877	41.2368	41.3114	41.2852	41.2518	41.3109	41.2273	41.2358
$\mathbb{V}[I(\theta)]$	0.2772	0.6958	0.9766	0.3466	0.8692	1.22	0.3984	0.9976	1.4044

Table 1. Mean value and variance for different values of a and α

Contrary to the mean value $\mathbb{E}[I(\theta)]$, it is noticeable that variance $\mathbb{V}[I(\theta)]$ of the quantity of interest is hardly sensitive the randomness. In addition, the values given in Tab. 1 underline that the parameter α has a strong impact on the severity of the problem: for all the considered values of a, the larger α, the larger the standard deviation. The same observation stands for parameter a: for all the values of α, the standard deviation increases as a increases.

Probability density functions (PDF) obtained with Monte-Carlo simulations are depicted in Figs. 3(a), 3(b) and 3(c). In fact, PDF are evaluated numerically and then we only obtain histograms corresponding to the PDF which are continuous. These histograms or discrete PDF are referred to as the reference solutions in the following sections.

Application of the proposed strategy

In this section, the numerical behavior of the proposed numerical strategy is assessed for different values of maximum admissible errors $\varepsilon_0 \in \{10^0; 10^{-1}; 10^{-2}; 10^{-3}; 10^{-4}\}$°C. This admissible error is the error between reduced basis and reference solution (discrete). As long as the same mesh is used, the discretization error due to the mesh does not influence the analysis. First of all, the discrete PDF of the quantity of interest are computed for three couples of parameters $(a,\ \alpha)$: $(0.25L_0,\ 2\%)$, $(0.5L_0,\ 5\%)$ and

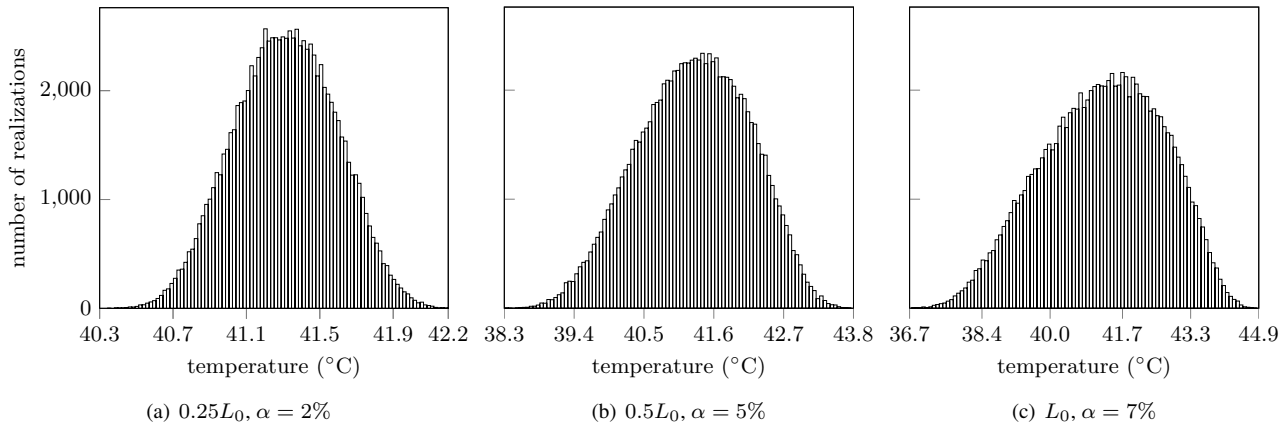

(a) $0.25L_0, \alpha = 2\%$ (b) $0.5L_0, \alpha = 5\%$ (c) $L_0, \alpha = 7\%$

Figure 3. Reference solutions: discrete PDF obtained with Monte-Carlo simulations

$(L_0,\ 7\%)$. These discrete PDF are respectively pictured in Figs. 4, 5 and 6. For each of these discrete PDF, their sensitivity to the

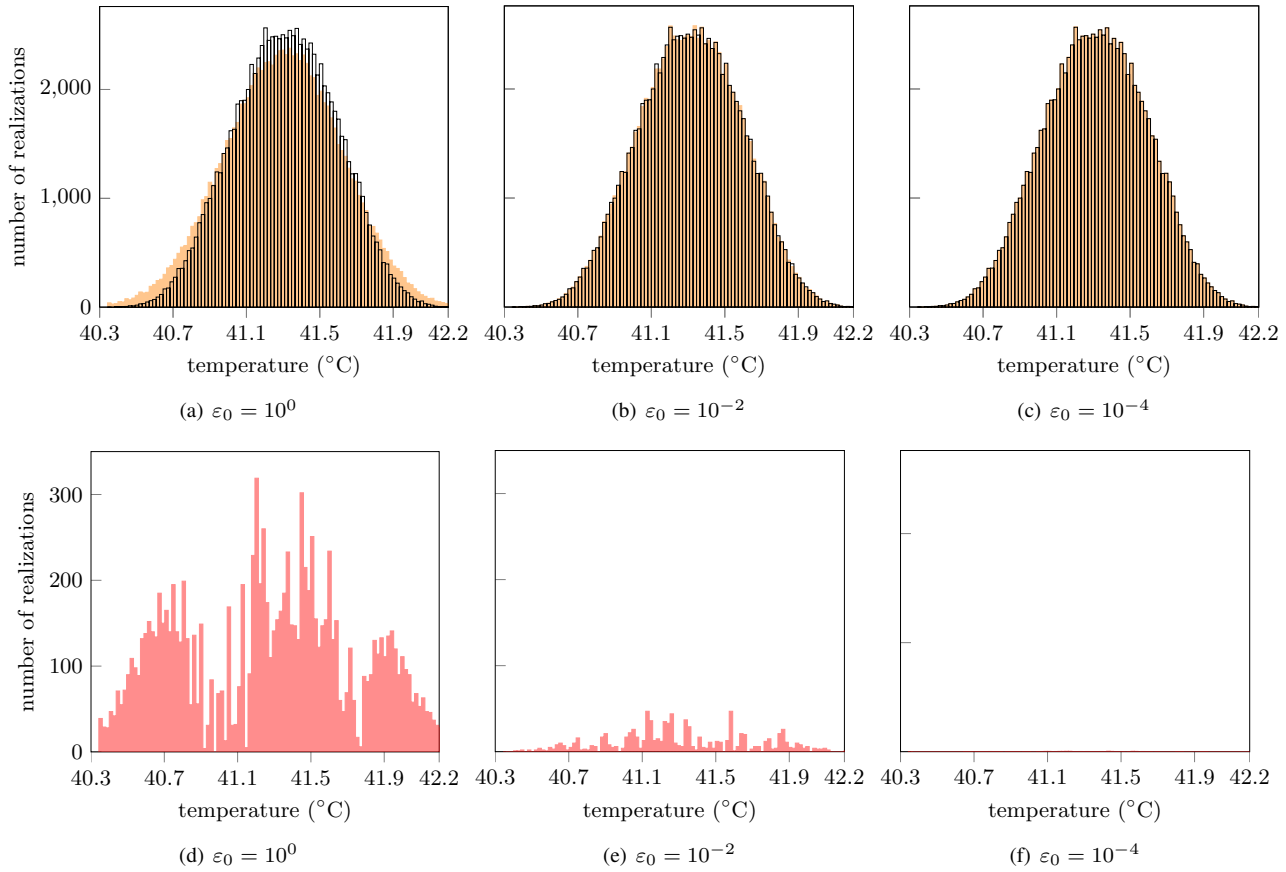

(a) $\varepsilon_0 = 10^0$ (b) $\varepsilon_0 = 10^{-2}$ (c) $\varepsilon_0 = 10^{-4}$

(d) $\varepsilon_0 = 10^0$ (e) $\varepsilon_0 = 10^{-2}$ (f) $\varepsilon_0 = 10^{-4}$

Figure 4. discrete PDF obtained with the proposed strategy (——) superimposed with those obtained with Monte-Carlo simulations (——) for $a = 0.25L_0$ and $\alpha = 2\ \%$. Corresponding errors are pictured in (——).

maximum admissible error is highlighted: the discrete PDF are shown for $\varepsilon_0 = 10^{0}$°C, $\varepsilon_0 = 10^{-2}$°C and $\varepsilon_0 = 10^{-4}$°C. For the sake of comparison, these discrete PDF are superimposed with the reference solution. For the sake of readability, differences between distributions obtained with the proposed strategy and Monte-Carlo simulations are also plotted. As the maximum admissible error is decreased, it is evidenced that the discrete PDF obtained with the proposed numerical strategy are perfectly superimposed with the reference solutions for any couple of parameters $(a,\ \alpha)$. In addition to these discrete PDF, the error between the reference solution and the proposed numerical strategy is computed for each realization. The maximal error $e_{\max}$ reported for each set of parameters ε_0, a and α is then reported in Tab. 2. The values given in Tab. 2 underline the quality of the proposed numerical strategy: the maximal error is comparable to the maximum admissible error ε_0 for almost all the couples of parameters $(a,\ \alpha)$ thus validating the error assessment procedure presented in this article. A more thorough analysis of the error committed with the proposed numerical strategy is carried out by plotting the discrete PDF of the error associated with the discrete PDF depicted above for the three couples of parameters $(a,\ \alpha)$: $(0.25L_0,\ 2\%)$, $(0.5L_0,\ 5\%)$ and $(L_0,\ 7\%)$. These discrete PDF are respectively pictured in Figs. 7, 8 and 9. These discrete PDF show that for almost all the realizations, the error is below the maximum admissible error. Though, in a few rare cases, the error assessment procedure fails to give an accurate result which is evidenced in Fig. 8(c) where one out of 10^5 realizations leads to an

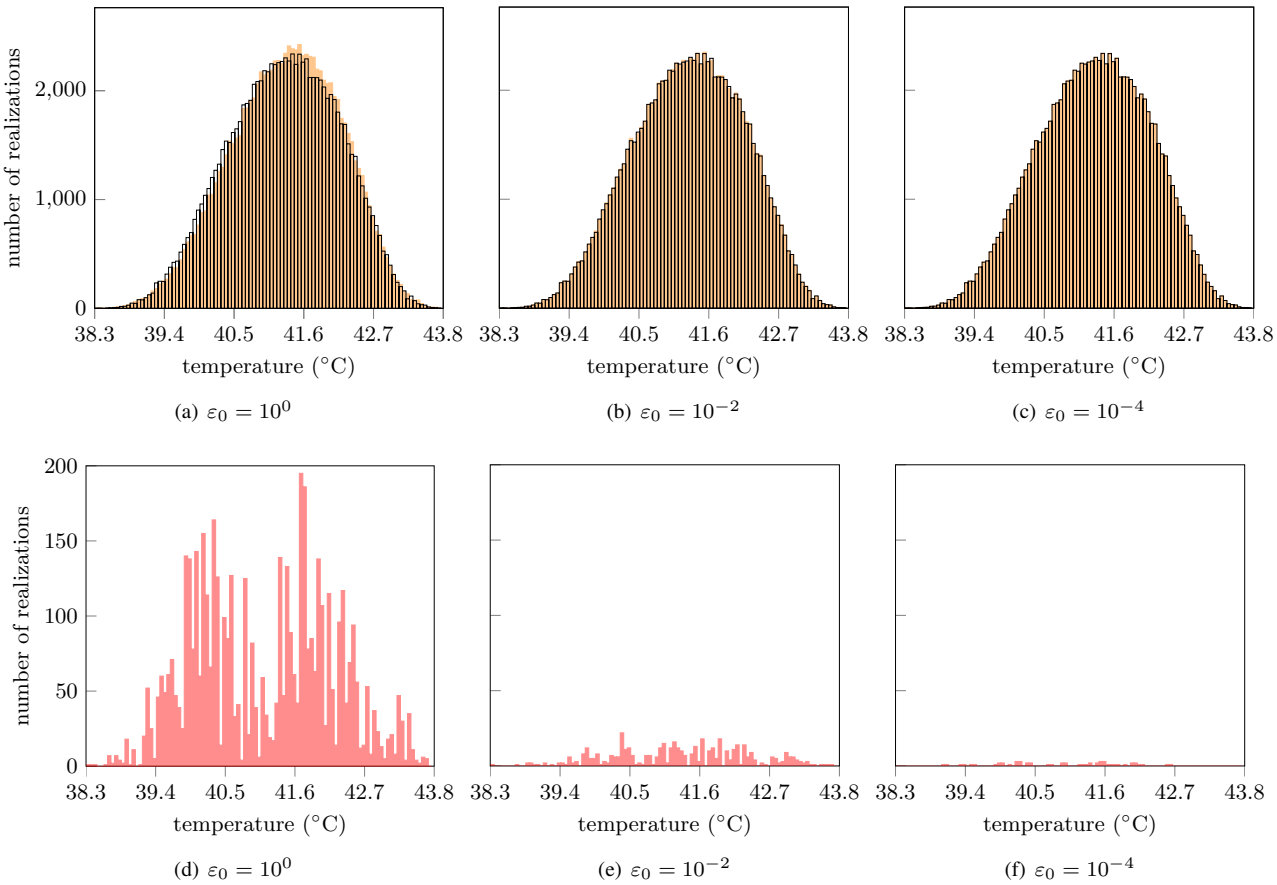

Figure 5. discrete PDF obtained with the proposed strategy (——) superimposed with those obtained with Monte-Carlo simulations (——) for $a = 0.5L_0$ and $\alpha = 5$ %. Corresponding errors are pictured in (——).

a	$0.25L_0$			$0.5L_0$			L_0		
ε_0 \ α	2%	5%	7%	2%	5%	7%	2%	5%	7%
10^0	0.98	0.95	0.94	0.9	1.03	0.86	0.82	0.84	0.91
10^{-1}	0.088	0.086	0.104	0.095	0.10	0.10	0.09	0.096	0.0114
10^{-2}	0.0099	0.0098	0.011	0.0095	0.0098	0.0107	0.0095	0.0103	0.0103
10^{-3}	0.00098	0.001	0.001	0.001	0.001	0.0013	0.001	0.001	0.001
10^{-4}	0.00018	0.00019	0.00017	0.00009	0.00069	0.00011	0.0000097	0.00012	0.00011

Table 2. Maximum error e_{max} for all the carried out simulations

error more than six times larger than the maximum admissible error (and thus explains the maximum error $e_{\max} = 0.00069 > 0.0001$ mentioned in Tab. 2 for $a = 0.5L_0$, $\alpha = 5$ % and $\varepsilon_0 = 10^{-4}$°C where $e_{max} = \max_{k\in[1..N_{MC}]} e(\theta_k)$). One can avoid these rare (less than 10 over 10^5) points (greater than ϵ_0) to define a more reasonable "maximum error" using probability bounds as in [38].

In order to be satisfying, the error assessment procedure must lead to a maximum error $e_{\max}$ that is as close as possible from the maximum admissible error ε_0. On the one hand, if the maximum error is too small, the algorithm is potentially too strict meaning that its numerical efficacy is not optimal. On the other hand, if the maximum error is too big, the approximation on the error assessment (39) is too permissive, see Fig. 10. In the end, the results presented in this section show that the proposed numerical strategy provides satisfying results: it does indeed allow for an accurate control of the maximum error when the parameters of the initial problem are perturbed.

Reduced basis evolution

This section focuses on the evolution of the reduced basis dimension during a simulation. In order to be computationally efficient, the final dimension of the reduced basis must remain small with respect to the dimension of the initial problem. It was evidenced in previous work [25] that the proposed methodology may yield a very significant decrease of computation times. Table 3 sums up the dimension of the reduced basis at the end of the simulations carried out for each set of parameters a, α and ε_0. It seems natural to witness an increase of the reduced basis dimension as the problem becomes more severe with increasing values of α. Similarly, it is observed that the smaller the maximum admissible error ε_0, the larger the dimension of the reduced basis. The dimensions listed in Tab. 3 should be compared with the dimension of the initial finite element problem which contains $N_{dof} = 441$ degrees of freedom solved on $N = 120$ time steps.

Before the reduced basis reaches its final dimension, a very large number of realizations are computed with even smaller bases. In order to better apprehend the way the reduced basis is enriched through out the computation of all the realizations, the dimension of

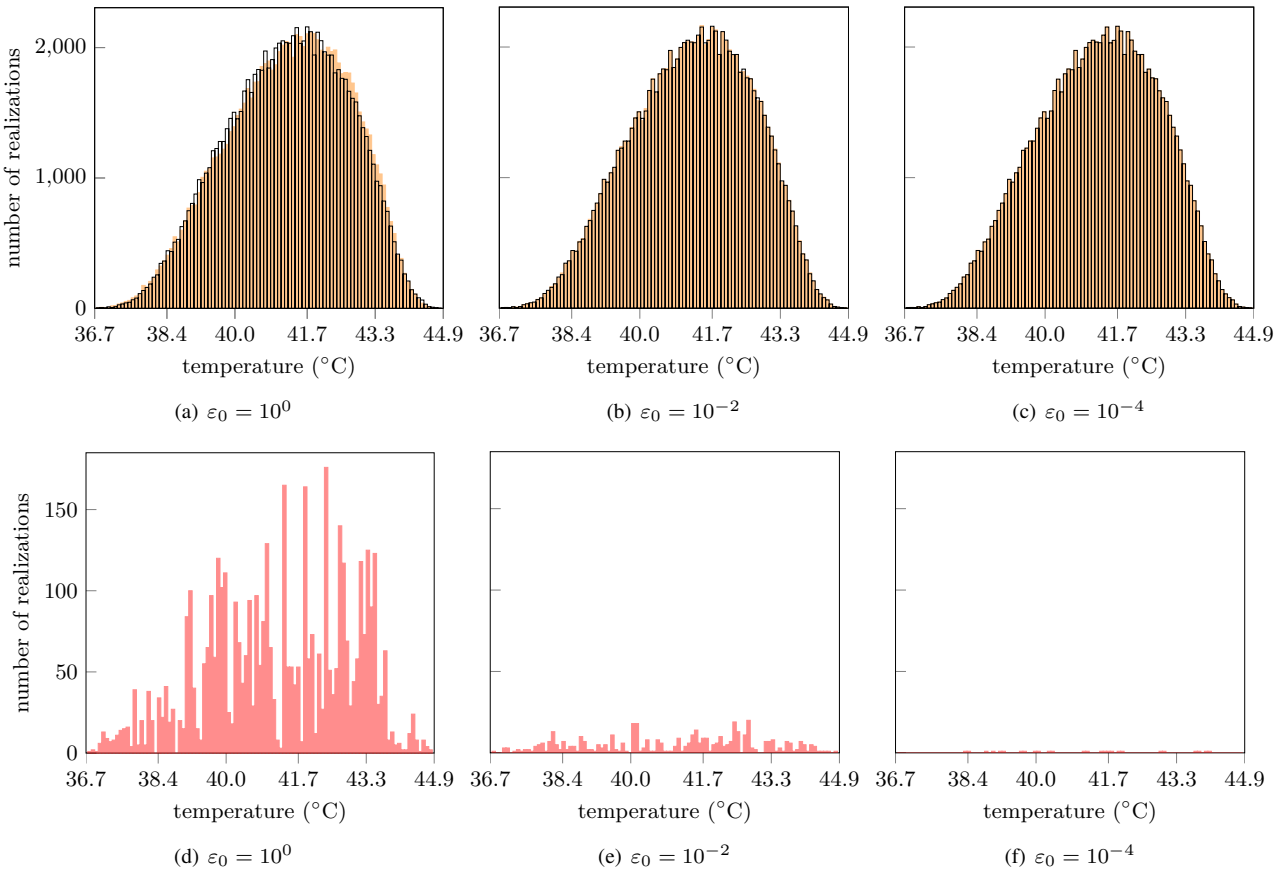

Figure 6. discrete PDF obtained with the proposed strategy (——) superimposed with those obtained with Monte-Carlo simulations (——) for $a = L_0$ and $\alpha = 7\ \%$. Corresponding errors are pictured in (——).

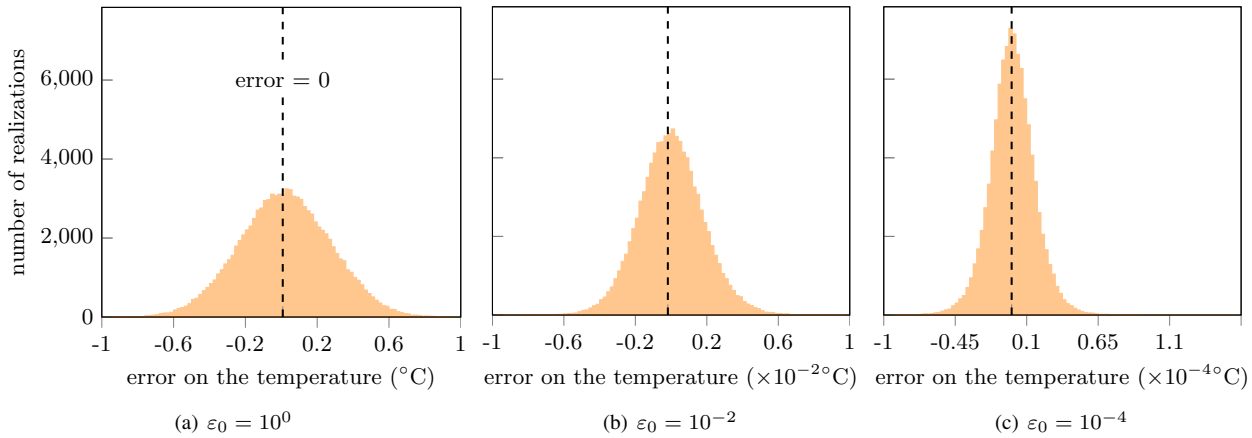

Figure 7. discrete PDF of the error for $a = 0.25L_0$ and $\alpha = 2\ \%$

a	$0.25L_0$			$0.5L_0$			L_0		
ε_0 \ α	2%	5%	7%	2%	5%	7%	2%	5%	7%
10^0	7	11	14	6	9	10	5	9	10
10^{-1}	15	21	32	16	21	23	15	19	20
10^{-2}	23	64	81	24	56	73	23	45	63
10^{-3}	72	131	167	63	120	151	56	108	130
10^{-4}	141	247	354	129	219	296	113	188	244

Table 3. Dimension of the reduced basis at the end of each simulation

the reduced basis is plotted with respect to the realization number in Figs. 11. For any set of parameters, the graphs drawn in Fig. 11 show that the reduced basis dimension is practically constant after the first 10 000 realizations. In other words, about 90 % of the realizations are computed with the final reduced basis which is constituted of a low number of selected vectors. Only the suitable vectors are kept in the basis, this small amount of vectors are sufficient to represent the variability of the problem. This illustrates the interest of the proposed method.

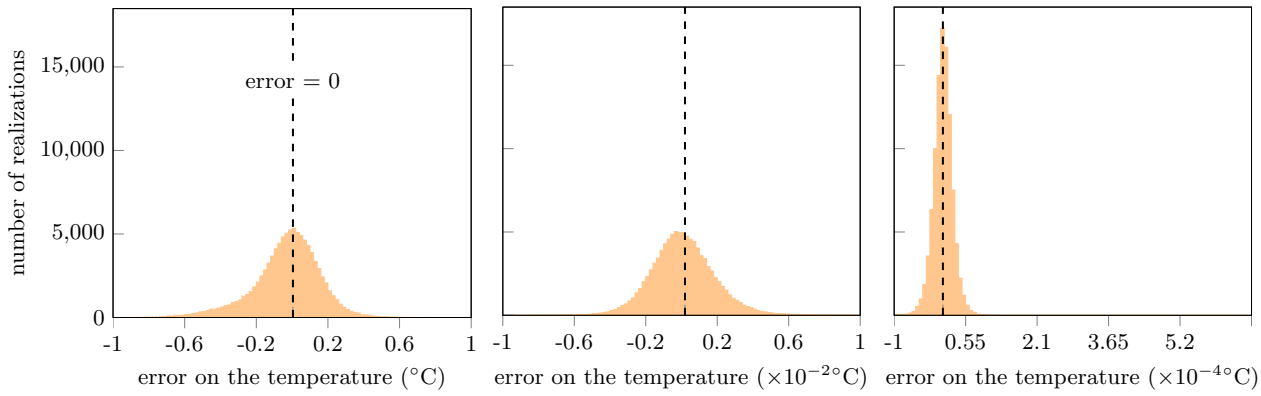

(a) $\varepsilon_0 = 10^0$ (b) $\varepsilon_0 = 10^{-2}$ (c) $\varepsilon_0 = 10^{-4}$

Figure 8. discrete PDF of the error for $a = 0.5L_0$ and $\alpha = 5\ \%$

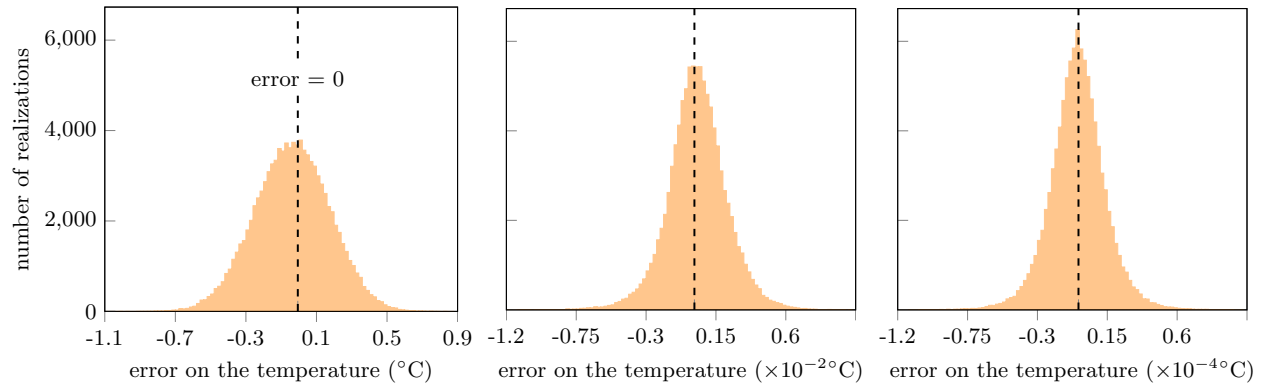

(a) $\varepsilon_0 = 10^0$ (b) $\varepsilon_0 = 10^{-2}$ (c) $\varepsilon_0 = 10^{-4}$

Figure 9. discrete PDF of the error for $a = L_0$ and $\alpha = 7\ \%$

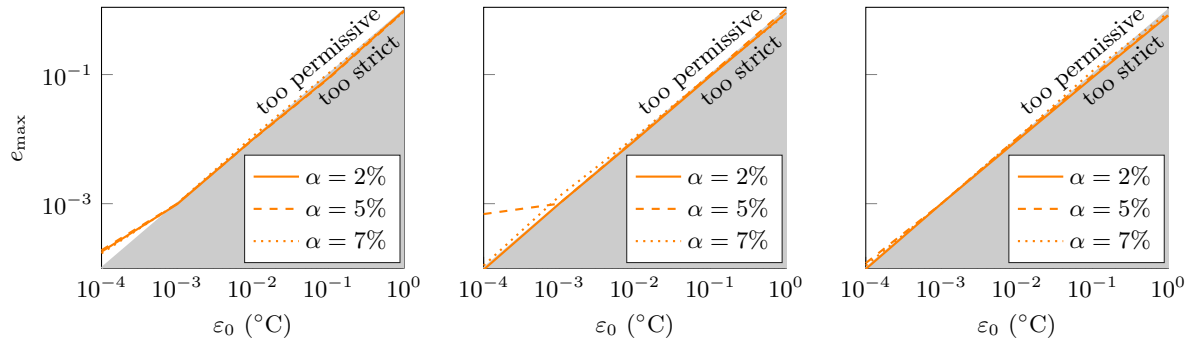

(a) $a = 0.25L_0$ (b) $a = 0.5L_0$ (c) $a = L_0$

Figure 10. Representation of the maximum error $e_{\max}$ with respect to the admissible maximum error ε_0

5. Conclusion

An original adaptive reduced basis technique is presented in this article. It is dedicated to the solution of nonstationary stochastic thermal problems. The cornerstone of the proposed strategy lies in an error assessment procedure that drives the modal content of the reduced basis. This strategy conveniently allows for the definition of a maximum admissible error and thus does not limit the dimension of the reduced basis. Following an extensive presentation of the theoretical background of the method, the adaptive reduced basis technique is applied on a test case which allows for a direct confrontation with usual Monte-Carlo simulations. Both the quality of the obtained results and the numerical efficacy of the proposed method are underlined through this example.

The proposed method shows great potential for the numerical analysis of stochastic problems and work is in progress for its application to the vibration analysis of structures undergoing random excitations. Future potential applications also include the analysis of large nonlinear frictional contact problems and the impact of manufacturing uncertainties over industrial structures free vibration modes. In such cases, defining such Adaptive Reduced Basis strategy is a challenge. Another challenging problem is to introduce variability on the geometry.

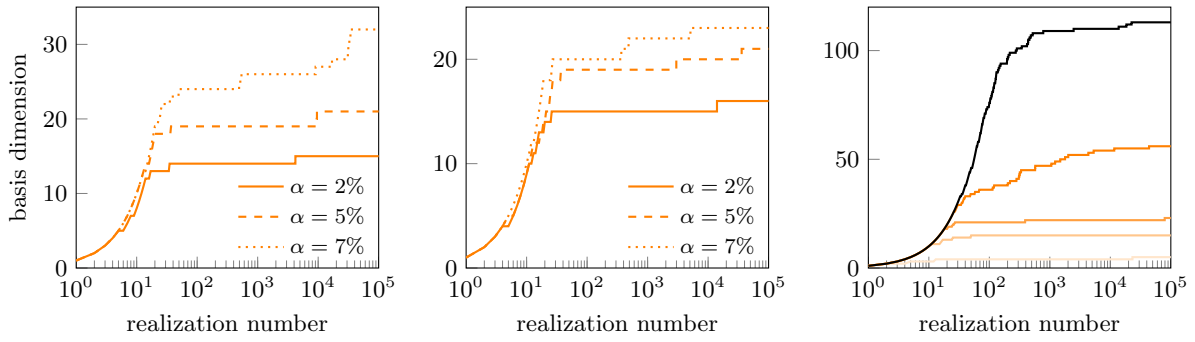

(a) $a = 0.25L_0, \varepsilon_0 = 10^{-1}$ (b) $a = 0.5L_0, \varepsilon_0 = 10^{-1}$ (c) $a = L_0, \alpha = 2\ \%, \varepsilon_0 = 10^{0}$ (——) to $\varepsilon_0 = 10^{-4}$ (——)

Figure 11. Reduced basis dimension for selected simulations

References

[1] S.-H. Lim, R. Bladh, M. P. Castanier, C. Pierre, Compact, generalized component mode mistuning representation for modeling bladed disk vibration, AIAA Journal 45 (2007) 2285 – 2297. doi:http://dx.doi.org/10.2514/1.13172.

[2] F. Nyssen, J.-C. Golinval, Identification of mistuning and model updating of an academic blisk based on geometry and vibration measurements, Mechanical Systems and Signal Processing 68 - 69 (2016) 252 – 264. doi:http://dx.doi.org/10.1016/j.ymssp.2015.08.006.

[3] C. Soize, Random matrix theory and non-parametric model of random uncertainties in vibration analysis, Journal of Sound and Vibration 263 (4) (2003) 893 – 916. doi:http://dx.doi.org/10.1016/S0022-460X(02)01170-7.

[4] G. I. Schueller, A state-of-the-art report on computational stochastic mechanics, Probabilistic Engineering Mechanics 12 (4) (1997) 197 – 321, a State-of-the-Art Report on Computational Stochastic Mechanics.

[5] A. Nouy, Recent developments in spectral stochastic methods for the numerical solution of stochastic partial differential equations, Archives of Computational Methods in Engineering 16 (2009) 251–285.

[6] G. Stefanou, The stochastic finite element method: Past, present and future, Computer Methods in Applied Mechanics and Engineering 198 (9-12) (2009) 1031 – 1051.

[7] R. Ghanem, P. Spanos, Stochastic Finite Elements: A Spectral Approach, Springer, 1991.

[8] M. K. Deb, I. M. Babuska, J. T. Oden, Solution of stochastic partial differential equations using galerkin finite element techniques, Computer Methods in Applied Mechanics and Engineering 190 (48) (2001) 6359 – 6372.
URL http://www.sciencedirect.com/science/article/pii/S0045782501002377

[9] H. G. Matthies, A. Keese, Galerkin methods for linear and nonlinear elliptic stochastic partial differential equations, Computer Methods in Applied Mechanics and Engineering 194 (12-16) (2005) 1295 – 1331, special Issue on Computational Methods in Stochastic Mechanics and Reliability Analysis.
URL http://www.sciencedirect.com/science/article/pii/S0045782504003950

[10] I. Babuska, R. Tempone, G. E. Zouraris, Solving elliptic boundary value problems with uncertain coefficients by the finite element method: the stochastic formulation, Computer Methods in Applied Mechanics and Engineering 194 (12-16) (2005) 1251 – 1294, special Issue on Computational Methods in Stochastic Mechanics and Reliability Analysis.
URL http://www.sciencedirect.com/science/article/pii/S0045782504003949

[11] M. F. Pellissetti, R. G. Ghanem, Iterative solution of systems of linear equations arising in the context of stochastic finite elements, Advances in Engineering Software 31 (8-9) (2000) 607 – 616.

[12] R. G. Ghanem, R. M. Kruger, Numerical solution of spectral stochastic finite element systems, Computer Methods in Applied Mechanics and Engineering 129 (3) (1996) 289 – 303.

[13] A. Keese, H. G. Matthies, Hierarchical parallelisation for the solution of stochastic finite element equations, Computers and Structures 83 (14) (2005) 1033 – 1047, uncertainties in Structural Mechanics and Analysis-Computational Methods.

[14] A. Doostan, R. G. Ghanem, J. Red-Horse, Stochastic model reduction for chaos representations, Computer Methods in Applied Mechanics and Engineering 196 (37-40) (2007) 3951 – 3966, special Issue Honoring the 80th Birthday of Professor Ivo Babuska.

[15] A. Nouy, Generalized spectral decomposition method for solving stochastic finite element equations: Invariant subspace problem and dedicated algorithms, Computer Methods in Applied Mechanics and Engineering 197 (51-52) (2008) 4718 – 4736.

[16] M. Papadrakakis, V. Papadopoulos, Robust and efficient methods for stochastic finite element analysis using monte carlo simulation, Computer Methods in Applied Mechanics and Engineering 134 (3-4) (1996) 325 – 340.

[17] S. Boyaval, C. L. Bris, Y. Maday, N. C. Nguyen, A. T. Patera, A reduced basis approach for variational problems with stochastic parameters: Application to heat conduction with variable robin coefficient, Computer Methods in Applied Mechanics and

Engineering 198 (41-44) (2009) 3187 – 3206. doi:DOI:10.1016/j.cma.2009.05.019.
URL http://www.sciencedirect.com/science/article/pii/S0045782509002114

[18] S. Boyaval, C. L. Bris, T. Lelièvre, Y. Maday, N. C. Nguyen, A. T. Patera, Reduced basis techniques for stochastic problems, Archives of Computational Methods in Engineering 17 (4) (2010) 435–454.

[19] S. Boyaval, A fast monte carlo method with a reduced basis of control variates applied to uncertainty propagation and bayesian estimation, Computer Methods in Applied Mechanics and Engineering 241–244 (2012) 190 – 205.

[20] L. Gallimard, D. Ryckelynck, A posteriori global error estimator based on the error in the constitutive relation for reduced basis approximation of parametrized linear elastic problems, Applied Mathematical Modelling 40 (7–8) (2016) 4271 – 4284. doi:http://dx.doi.org/10.1016/j.apm.2015.11.016.
URL http://www.sciencedirect.com/science/article/pii/S0307904X15007301

[21] R. Cottereau, P. Díez, Fast r-adaptivity for multiple queries of heterogeneous stochastic material fields, Computational Mechanics 56 (4) (2015) 601–612. doi:10.1007/s00466-015-1190-x.
URL http://dx.doi.org/10.1007/s00466-015-1190-x

[22] I. Bianchini, R. Argiento, F. Auricchio, E. Lanzarone, Efficient uncertainty quantification in stochastic finite element analysis based on functional principal components, Computational Mechanics 56 (3) (2015) 533–549.

[23] F. Louf, L. Champaney, Fast validation of stochastic structural models using a {PGD} reduction scheme, Finite Elements in Analysis and Design 70-71 (2013) 44 – 56. doi:http://dx.doi.org/10.1016/j.finel.2013.04.003.

[24] E. Florentin, P. Díez, Adaptive reduced basis strategy based on goal oriented error assessment for stochastic problems, Computer Methods in Applied Mechanics and Engineering 225-228 (0) (2012) 116 – 127.

[25] K. Serafin, B. Magnain, E. Florentin, N. Parés, P. Díez, Enhanced goal-oriented error assessment and computational strategies in adaptive reduced basis solver for stochastic problems, International Journal for Numerical Methods in Engineering Accepted in august 2016. doi:http://dx.doi.org/10.1002/nme.5363.

[26] A. Emery, Solving stochastic heat transfer problems, Engineering Analysis with Boundary Elements 28 (3) (2004) 279 – 291, inverse Problems. doi:http://dx.doi.org/10.1016/S0955-7997(03)00058-4.
URL http://www.sciencedirect.com/science/article/pii/S0955799703000584

[27] F. Wu, W. Zhong, A modified stochastic perturbation method for stochastic hyperbolic heat conduction problems, Computer Methods in Applied Mechanics and Engineering 305 (2016) 739 – 758. doi:http://dx.doi.org/10.1016/j.cma.2016.03.032.
URL http://www.sciencedirect.com/science/article/pii/S0045782516301177

[28] M. Loève, Fonctions aléatoires du second ordre, Comptes Rendus de l'Académie des Sciences - Paris 220 (1945) 380–382.

[29] K. Karhunen, Uber lineare methoden in der wahrscheinlichkeitsrechnung, Amer. Acad. Sci., Fennicade (Translation: RAND Corporation, Santa Monica, California, Rep. T-131, Aug. 1960). 37 (1947) 3–79.

[30] L. Chamoin, E. Florentin, S. Pavot, V. Visseq, Robust goal-oriented error estimation based on the constitutive relation error for stochastic problems, Computers and Structures 106–107 (2012) 189 – 195. doi:http://dx.doi.org/10.1016/j.compstruc.2012.05.002.
URL http://www.sciencedirect.com/science/article/pii/S0045794912001198

[31] P. Ladevèze, B. Blaysat, É. Florentin, Strict upper bounds of the error in calculated outputs of interest for plasticity problems, Computer Methods in Applied Mechanics and Engineering 245–246 (2012) 194 – 205. doi:http://dx.doi.org/10.1016/j.cma.2012.07.009.
URL http://www.sciencedirect.com/science/article/pii/S0045782512002290

[32] E. Florentin, S. Guinard, P. Pasquet, A simple estimator for stress errors dedicated to large elastic finite element simulations Locally reinforced stress construction, Engineering Computations 28 (1-2) (2011) 76–92.

[33] K. Kunisch, S. Volkwein, Galerkin proper orthogonal decomposition methods for parabolic problems, Numer Math 90. doi:10.1007/s002110100282.
URL http://dx.doi.org/10.1007/s002110100282

[34] S. Sanghi, N. Hasan, Proper orthogonal decomposition and its applications, Asia Pac J Chem Eng 6. doi:10.1002/apj.481.
URL http://dx.doi.org/10.1002/apj.481

[35] Y. Maday, E. Rønquist, A reduced-basis element method, J Sci Comput 17. doi:10.1023/A:1015197908587.
URL http://dx.doi.org/10.1023/A:1015197908587

[36] G. Rozza, D. B. P. Huynh, A. T. Patera, Reduced basis approximation and a posteriori error estimation for affinely parametrized elliptic coercive partial differential equations, Arch Comput Methods Eng 15. doi:10.1007/s11831-008-9019-9.
URL http://dx.doi.org/10.1007/s11831-008-9019-9

[37] R. Becker, R. Rannacher, An optimal control approach to a posteriori error estimation in finite element methods, Acta Numerica 10 (2001) 1–120.

[38] F. Louf, P. Enjalbert, P. Ladeveze, T. Romeuf, On lack-of-knowledge theory in structural mechanics, Comptes Rendus Mécanique 338 (7) (2010) 424 – 433. doi:http://dx.doi.org/10.1016/j.crme.2010.07.012.